Asian Journal of Pharmaceutical Sciences 18 (2023) 100848

Available online at www.sciencedirect.com

ScienceDirect

journal homepage: www.elsevier.com/locate/AJPS

Original Research Paper

Comparison of virus-capsid mimicking biologic-shell based versus polymeric-shell nanoparticles for enhanced oral insulin delivery ☆

Zhixiang Cui[a], *Shuman Cui*[a], *Lu Qin*[a], *Yalin An*[a], *Xin Zhang*[a], *Jian Guan*[a], *Tin Wui Wong*[b,c], *Shirui Mao*[a,*]

[a] *School of Pharmacy, Shenyang Pharmaceutical University, Shenyang 110016, China*
[b] *Particle Design Research Group, Faculty of Pharmacy, Universiti Teknologi MARA Selangor, Puncak Alam 42300, Malaysia*
[c] *Non-Destructive Biomedical and Pharmaceutical Research Centre, Smart Manufacturing Research Institute, Universiti Teknologi MARA Selangor, Puncak Alam 42300, Malaysia*

ARTICLE INFO

Article history:
Received 23 March 2023
Revised 15 August 2023
Accepted 11 September 2023
Available online 24 September 2023

Keywords:
Oral insulin
Streptavidin
Virus-mimicking
Nanoparticles
Muco-penetrating
Mucus

ABSTRACT

Virus-capsid mimicking mucus-permeable nanoparticles are promising oral insulin carriers which surmount intestinal mucus barrier. However, the impact of different virus-capsid mimicking structure remains unexplored. In this study, utilizing biotin grafted chitosan as the main skeleton, virus-mimicking nanoparticles endowed with biologic-shell (streptavidin coverage) and polymeric-shell (hyaluronic acid/alginate coating) were designed with insulin as a model drug by self-assembly processes. It was demonstrated that biologic-shell mimicking nanoparticles exhibited a higher intestinal trans-mucus (>80%, 10 min) and transmucosal penetration efficiency (1.6–2.2-fold improvement) than polymeric-shell counterparts. Uptake mechanism studies revealed caveolae-mediated endocytosis was responsible for the absorption of biologic-shell mimicking nanoparticles whereas polymeric-shell mimicking nanoparticles were characterized by clathrin-mediated pathway with anticipated lysosomal insulin digestion. Further, *in vivo* hypoglycemic study indicated that the improved effect of regulating blood sugar levels was virus-capsid structure dependent out of which biologic-shell mimicking nanoparticles presented the best performance (5.1%). Although the findings of this study are encouraging, much more work is required to meet the standards of clinical translation. Taken together, we highlight the external structural dependence of virus-capsid mimicking nanoparticles on the muco-penetrating and uptake mechanism of enterocytes that in turn affecting their *in vivo* absorption, which should be pondered when engineering virus-mimicking nanoparticles for oral insulin delivery.

☆ Peer review under responsibility of Shenyang Pharmaceutical University.

* Corresponding author.
E-mail address: maoshirui@syphu.edu.cn (S. Mao).
Peer review under responsibility of Shenyang Pharmaceutical University.

https://doi.org/10.1016/j.ajps.2023.100848

1. Introduction

Diabetes mellitus, as the third greatest cause of mortality in the world, is a chronic disease characterized by metabolic disorders and elevated blood glucose levels [1]. Since the majority of patients with diabetes are diagnosed with Type II, the most effective treatment available relies exclusively on insulin injection in the subcutaneous tissue to regulate their blood glucose levels. Yet, the attendant adverse effects from parenteral administration are poor compliance, lipoatrophy occurring at the injection site, and even risky hypoglycemia [2,3]. Oral insulin delivery, by contrast, is a preferred route of administration due to its convenience and circumvention of frequent injections. Importantly, oral insulin can imitate the physiological route of endogenous insulin secretion, facilitating the maintenance of glucose homeostasis. However, currently oral bioavailability of insulin shows inferior consequences (<1%), owing to its physicochemical properties (large molecular weight, high hydrophilicity, and poor physicochemical stability), which make it difficult to be absorbed orally. In addition, the formulations must overcome a variety of barriers, primarily mucus and intestinal epithelium [4].

Over the past few years, vast efforts have been devoted to exploring feasible strategies for raising peroral insulin absorption. Among them, nanoparticles (NPs) showed distinctive advantages including enhancing drug stability in the hostile gastrointestinal milieu, facilitating cargo transmembrane transit and elevating medication bioavailability [5]. Moreover, the innovation of manifold materials applied for NPs construction spurred the advancement of various delivery systems, especially muco-penetrating based, which are more conducive to delivering a payload to access the underlying epithelial tissues by overcoming the mucus lining barrier, thereby strengthening the therapeutic efficiency over conventional mucoadhesion systems [6]. On this note, PEGylation is the gold standard strategy to improve the mucus inertness of NPs, which serves as a benchmark for copolymers used in nano-delivery systems [7]. Poly (ethylene glycol) (PEG) as hydrophilic and biocompatible polymer has been ubiquitously leveraged to conjugate with therapeutic agents or decorate on the surface of NPs, which is known as PEGylation. Apart from the stability and biocompatibility of PEGylated nanosystems can be greatly enhanced, the resulting "brush" corona configuration would facilitate penetration of the PEGylated particles through the mucus lining. Nonetheless, considering the consequence of compromising the subsequent cellular uptake and immune response of PEGylated NPs, the development of alternative muco-penetrating strategies is of a requisite.

It was reported that many viruses could traverse rapidly through mucus, benefiting from their peculiar surface characteristics, i.e., a hydrophilic surface wrapped by a high density of cationic and anionic moieties, which reduced their interaction with mucus and conferred effective transport across epithelial cells [8]. The characteristics of viruses served as inspiration for our team as they created the virus-mimicking NPs to overcome the mucus barrier. For example, muco-inert nanocomplexes were fabricated by coating biotinylated chitosan (CS-Biotin$_{21.8\%}$) with hyaluronic acid (HA) where the optimal virus-mimicking structure was formed by HA with a molecular weight of 200 kDa, which showed excellent muco-penetration and enhanced oral absorption [9]. Likewise, an optimized core-shell structure with alginate (Alg, Manucol LD) coating illustrated the greatest permeation strengthening capacity in porcine mucus [10]. However, the enhanced muco-penetrating and oral bioavailability of NPs composed of a polymeric-shell were still unsatisfactory. Based on the universality of the virus-capsid mimicking concept, we hypothesized that using natural protein components to structure mucus-permeable NPs based on biologic-shell mimicking might be a better strategy to achieve biological mimicry of viral capsid both structurally and functionally simultaneously, and what's more, to enable enhanced mucus permeability and better absorption via oral administration.

Streptavidin (SA), a 56 kDa tetrameric protein derived from streptomyces, is the most typical analogue of avidin, which has been generally exploited as affinity matrices and probes for a broad spectrum of applications in delivery of medication, diagnosis and biochemical assays [11]. The mechanism of (strept)avidin-biotin interaction is considered as specific and robust non-covalent binding, which is about 103–106 times stronger than an antigen-antibody interaction. In addition, the biotin-avidin system can be easily manufactured without compromising the chemical and biological traits of the coupled moieties, making it a flexible platform for nanotechnology-based systems [12]. Consequently, an intelligent design of virus-mimicking NPs utilizing the biotin-SA system to closely resemble the surface characteristics of viral envelope to facilitate mucus penetration is interesting and promising. Furthermore, to the best of our knowledge, limited information is available regarding the structure influence of virus-capsid mimicking NPs on their *in vivo* fate, and thus a systematical comparison is absolutely essential to elucidate the implication of capsid-mimicking structure on their *in vitro* and *in vivo* performance.

As such, this paper's goal is to clarify the impact of different virus-capsid mimicking structures on oral insulin delivery. First of all, the nanocomplex core comprising CS-Biotin$_{21.8\%}$ and insulin was prepared by spontaneous self-assembly, followed by SA combination process and the biotin-SA interaction was confirmed by low-field NMR method. Similarly, polymeric-shell mimicking NPs were prepared by coating the nanocomplex with the optimized polymer (HA or Alg). Thereafter, the effect of different virus-capsid mimicking NPs structure on colloidal stability, *in vitro* mucodiffusion, *ex vivo* mucus retention, and intestinal permeability was investigated and contrasted systemically. Additionally, the mechanism of enterocyte endocytosis of different structured NPs was studied and compared, with *in vivo* hypoglycemic performance further evaluated.

2. Materials and methods

2.1. Materials

Porcine insulin was purchased from Wanbang Biochemical Pharmaceutical Company (China). Biotin modified chitosan with a grafting degree of 21.8% (CS-Biotin$_{21.8\%}$) was obtained by chemical synthesis according to the previous protocol [9]. Hyaluronic acid (HA, molecular weight = 200 kDa) was from Shanghai Bloomage Biotechnology Co., Ltd. (Shanghai, China). Alginate Manucol LD (Alg, molecular weight = 145 kDa, 37–40% G content) was donated by FMC Corporation as a gift. Polyglutamic acid (PGA, molecular weight = 50 kDa) was supplied by Shanghai Yuanye Biotechnology Co., Ltd. (Shanghai, China). Tris buffer, Cy5 monosuccinimidyl est. (Cy5-NHS), trypsin, DAPI solution and N-acetyl-L-cysteine (NAC) were acquired from Dalian Meilun Biotechnology Co., Ltd (Dalian, China). FITC was purchased from Little-PA Sciences Co., Ltd (China). Type II porcine stomach mucin was obtained from Sigma-Aldrich (Munich, Germany). The remaining compounds belonged to analytical grade.

2.2. Preparation and characterization of virus-mimicking NPs

Insulin loaded polyelectrolyte nanocomplexes based on CS-Biotin$_{21.8\%}$ copolymers were prepared in accordance with the prior approach [13]. In a nutshell, the pH of dissolved CS-Biotin$_{21.8\%}$ (1 mg/ml in 0.25% acetic acid) was set to 5.5, and the insulin stock solution (1 mg/ml, pH 7.8) was obtained using 87% (v/v) 0.01 N HCl and 13% (v/v) 0.1 N Tris buffer. Afterwards, 1 ml insulin solution was introduced into an equal volume of CS-Biotin$_{21.8\%}$ solution in a dropwise manner under continuous magnetic stirring (120 rpm) for 25 min, resulting in the formation of nanocomplexes.

For the preparation of biologic-shell mimicking NPs based on biotin-SA combination, the interaction process was completed by adding a certain mole ratio of SA (0.1 mg/ml, 8/17/35/70 µl) to the nanocomplexes within 10 min of incubation, then 1 ml freshly prepared NPs was slowly added to the same volume of PGA (0.4 mg/ml) at pH 6. Following 10 min of incubation at ambient temperature, biologic-shell mimicking NPs with dense coverage of positive and negative charges were acquired. Likewise, for the preparation of polymeric-shell mimicking NPs based on polyanions-cations electrostatic interplay, the coating step was performed by adding 1 ml the freshly prepared nanocomplexes dropwise to the previously optimized 1.5 ml HA (200 kDa of 0.6 mg/ml) and 1 ml Alg (Manucol LD of 0.4 mg/ml) solutions, respectively.

Particle size and zeta potential (Z-ave) of the NPs were determined by DLS (Zetasizer NanoZS, Malvern Instruments, Germany). Morphology of the virus-capsid mimicking NPs was visualized using by TEM (FEI Tecnai G2 F30, USA). To measure insulin encapsulation efficiency (EE), samples were centrifuged at 14,000 rpm for 40 min (HC-2062, Ustc Zonkia Scientific Instruments, China) and then analyzed utilizing HPLC methodology to quantify insulin content in the supernatant [14], under the following conditions: column temperature of 40 °C, flow rate of 1 ml/min and detection wavelength of 214 nm. The mobile phase was made up of sulfate buffer (0.2 M, pH 2.5) and acetonitrile at a volume ratio of 500:205, and EE was calculated using the following equation:

$$\text{EE}\ (\%) = \frac{\text{Total quantity of added insulin} - \text{supernatant free insulin}}{\text{Total quantity of added insulin}} \times 100\%$$

2.3. Measurement of solvent relaxation NMR

Non-covalent specific interaction of biotin-SA and an optimum mole ratio of biotin to SA were determined via assessing the spin-spin relaxation time (T_2) of NPs using Acron area analyzer (XiGo Nanotools, USA), operating at 13 MHz. After completing instrument calibration with copper sulfate standard solution, the NMR tube containing 0.6 ml test solution was inserted into the sample tube orifice. The measurement was performed under the following conditions: Carr–Purcell–Meiboom–Gill (CPMG) pulse sequence with 625 echo cycles, $\tau = 0.5$ ms, 25 °C, anticipated T_2 value ±20%.

2.4. Virus-mimicking NPs stability study

2.4.1. Colloidal stability

Colloidal stability of the virus-capsid mimicking NPs in simulated intestinal medium (SIM; Trypsin 1% (w/v), KH_2PO_4 50 mM, NaOH 15 mM to pH 6.8) was examined. In brief, 1 ml the freshly prepared preparation was placed in 4 ml SIM and incubated under shaking (37 °C, 80 rpm) for 2 h. Afterwards, integrity of the NPs was monitored via particle size assessment [15].

2.4.2. Enzymatic stability

Capacity of the virus-capsid mimicking NPs to preserve insulin against enzymatic degradation was studied. In short, 500 µl insulin solution or different formulations were added to a pH 6.8 trypsin solution with a concentration of 0.1 M in Tris buffer (250 U/ml) of the same volume and incubated under air bath condition (37 °C, 80 rpm). Aliquots of 200 µl were withdrawn at scheduled time intervals (15/30/60/120 min) and the reaction was promptly halted by adding 100 µl 0.1 N hydrochloric acid solution. After the mixture was subjected to centrifugation (14,000 rpm, 30 min), the leftover insulin content in the supernatant was determined using HPLC method [16].

2.5. In vitro mucus diffusion study

The potential of virus-capsid mimicking NPs to infiltrate through the mucus lining was studied using the previously described approach [17]. Firstly, insulin labeled with FITC was synthesized as the previous protocol [18], followed by FITC-insulin loaded formulations preparation. Crude mucus was obtained from the swine's intestine and pre-treated as per the earlier report [10]. Then, 500 µl the FITC-insulin loaded NPs were incubated with the above treated mucus for 10 min at 37 °C in an air-bath oscillator (80 rpm). Thereafter, the samples were centrifuged for 10 min at 2000 rpm and a microplate reader (SpectraMax® M3 multiscan Spectrum, Molecular Devices Corporation, USA) was used to quantify the fluorescence intensity (FI) of the supernatant was detected (EX 480 nm, EM 530 nm). The percentage of virus-capsid

mimicking NPs permeated across mucus was calculated as followed:

$$\text{Mucus permeation percentage (\%)} = \frac{\text{FI in the mucus supernatant}}{\text{FI in the original solution}} \times 100\%$$

2.6. Transmucosal penetration and enterocyte influx mechanism study

In vitro study of intestinal epithelium permeation was conducted using freshly isolated small intestinal segments of male Sprague Dawley (SD) rats (body weight = 200 ± 20 g/rat, $n = 3$ per group) supplied by the Animal Center of Shenyang Pharmaceutical University, China. Also, all animal procedures described herein adhered to the Principle of Laboratory Animal Care and had been approved by the Ethics Committee, complied with the National Institutes of Health guide for the care and use of Laboratory animals (NIH Publications No. 8023, revised 1978) as well. Firstly, by mixing together 10 ml insulin solutions (4 mg/ml, 0.01 N HCL) with 400 l Cy5-NHS solution (0.25 mg/ml in DMSO) and stirring for 12 h in the dark, Cy5 labeled insulin was created. Until the dye was undetectable, unconjugated Cy5-NHS was eliminated by dialysis (Biotopped, MWCO 3000 Da). Then the resulting Cy5-insulin was subjected to NP formulation [19]. Prior to the experiment, the SD rats were fasted for a whole night with unlimited access to water. After the rats were euthanized by intraperitoneally administering an overdose of chloral hydrate, the duodenum, jejunum and ileum of rats were surgically cut (5 cm in length) and isolated. After that, per intestinal segments were directly administered into 0.5 ml Cy5-insulin loaded virus-capsid mimicking NPs, ligated at both ends, and immersed in 10 ml Krebs–Ringer (KR) solution (37 °C, 80 rpm). At regular time intervals, 600 µl the aliquots were draw out and further assayed by microplate reader, followed by KR supplement of an identical volume. The equation to calculate apparent permeability coefficient (P_{app}) was as followed:

$$P_{app} = \frac{dQ}{dt} \times \frac{1}{A \times C_0}$$

where dQ/dt is the flux of Cy5-insulin from the bowel cavity to KR medium, A and C_0 stand for the surface area of the intestinal segments and the initial concentration of Cy5-insulin respectively.

The enterocyte entry mechanism of virus-capsid mimicking NPs was examined by treating the rat jejunum with various metabolic inhibitors to block the related endocytic pathways namely indomethacin (caveolin inhibitor), colchicine (macropinocytosis inhibitor) and chlorpromazine (clathrin inhibitor). Besides, the investigated NPs were also introduced to the jejunum and incubated at 4 °C and 37 °C correspondingly with inhibitor-free, the subsequent procedures were identical to those outlined previously.

2.7. Intestinal retention and muco-penetration ex vivo study

The male SD rats (body weight: 200 ± 20 g/rat, $n = 3$ per group) were starved overnight before the experiment but had unrestricted access to water. During the experiment, intraperitoneal injections of 4% chloral hydrate were used to anesthetize the rats. Then a 5 cm loop of jejunum was knotted in place at both ends *in situ*. Following that, 300 µl Cy5-insulin loaded investigated NPs were injected into the treated jejunum. Upon incubation of 1 h, the rats were euthanized and the 5 cm treated jejunum segments were taken out surgically, subsequently underwent a gentle wash of normal saline. Then, the loops were cut open longitudinally and flattened to expose mucosal surface. The observation was taken using *in vivo* imaging device (Carestream FX PRO, USA), and the average fluorescence intensity was denoted as AFI_{before}. Next, the jejunum was submerged in 10% *N*-acetyl-L-cysteine solution and incubated for 30 min under shaking (37 °C, 80 rpm), followed by thrice rinsing to remove the mucus. Likewise, the average fluorescence intensity of treated jejunum was recorded (AFI_{after}). The permeability efficiency of the virus-capsid mimicking NPs was expressed via the following equation [20]:

$$\text{Permeability efficiency (\%)} = \frac{AFI_{after}}{AFI_{before}} \times 100\%$$

Further, uptake of the virus-capsid mimicking NPs in rat enterocytes was studied utilizing the multi-photon confocal microscope (LSM 710, Zeiss, Germany). The jejunum loop tissue was gently rinsed with normal saline, fixed for two hours in 10 ml 4% paraformaldehyde, and then kept in 10 ml 30% sucrose solution overnight at 4 °C. The loop tissue was frozen with O.C.T. compound and sectioned into 10 µm thickness. DAPI solution was employed to stain the nucleus of enterocytes.

2.8. In vivo hypoglycemic level

Therapeutic efficacy of various formulations was contrasted based on *in vivo* hypoglycemic study. Ahead of the experiment, male SD rats (body weight: 200 ± 20 g/rat, $n = 6$ per group) were fasted but free to water overnight. Sodium bicarbonate was utilised to neutralize the stomach acid of rats before various formulations were administrated through oral gavage (50 IU/kg) [21]. A free insulin solution (2 IU/kg) was administered subcutaneously as a control. Blood samples were obtained from the rat's caudal veins before dosing and at the pre-set time points, the blood glucose level was monitored by a glucose meter (JPS-6, Yicheng Biotech. Co., Ltd Beijing, China). The following formula was used to compute the relative pharmacological availability (PA%):

$$\text{Relative PA (\%)} = \frac{AAC_{oral} * Dose_{sc}}{AAC_{sc} * Dose_{oral}} \times 100\%$$

where AAC is defined as the entire area from 0 to 10 h over the baseline blood glucose level, determined using the trapezoidal method.

2.9. Histopathological study

The histological study of intestinal biopsies was performed using male SD rats (body weight: 200 ± 20 g/rat) with the aim to test the *in vivo* safety of virus-capsid mimicking NPs. In brief,

the control and test groups were given normal saline or insulin loaded formulations orally once a day (50 IU/kg), respectively. The stomach, duodenum, jejunum, and ileum were removed from the rats after 7 d, carefully cleaned with physiological saline solution, preserved with 4% (w/v) paraformaldehyde, and then sliced into 5 μm thick paraffin sections. The paraffin slices were then viewed under a stereomicroscope after being stained with hematoxylin and eosin (H&E).

2.10. *Statistical analysis*

Unless otherwise specified, all experimental results are provided as mean ± standard deviation, with three independent measurements. GraphPad Prism 8 is used for statistical analysis, which includes the two-tail Student's *t*-test and one-way analysis of variance (ANOVA). Statistical differences were regarded when the *P* value was less than 0.05 ($P < 0.05$).

3. Results and discussion

3.1. *Preparation and characterization of virus-capsid mimicking NPs with different structure*

Chitosan (CS) is a desirable skeleton of nanocarrier for oral insulin delivery due to its tunable structure via chemical modification. Moreover, the biotin decorated CS copolymer with a biotin substitution degree of 21.8% has been identified as a potential carrier of insulin (CS-Biotin$_{21.8\%}$/Insulin), owing to its ability to overcome the mucus barrier in accordance with the recent study [8]. Hence, CS-Biotin$_{21.8\%}$/Insulin was herein selected as the nanocomplex core for further design of mucus-permeable NPs with various capsid-mimicking structure.

Inspired by the general applicability of the virus-mimicking concept, biologic-shell mimicking NPs were created based on the nanocomplex core via the robust interaction between biotin and SA to accomplish virus-capsid mimicking in terms of structure and function. First, the binding mole ratio of biotin and SA was optimized by low-field NMR. It can be seen that there was a similar T_2 value in the 8/1 group compared with CS-Biotin$_{21.8\%}$/Insulin ($P > 0.05$), indicating SA did not exist in free-state in the bulk solution but bounded with biotin modified chitosan (Fig. 1). Theoretically, based on the great affinity and specificity, each of four subunits in SA binds to biotin [22]. However, a significant increase in T_2 was observed when the biotin/SA ratio varied from 4/1 to 1/2 ($P < 0.05$), implying that unbound SA was partly available in the bulk solution. This result may be explained by the fact that a portion of the biotin ligands were buried in the interior of the nanocomplex core, resulting in incomplete theoretical combination. Therefore, the mole ratio of 8:1 was chosen for fabricating biologic-shell mimicking NPs. Considering the resultant NPs featured positive zeta potential, PGA was added to tune the surface charges to be comparable with the polymeric-shell mimicking one without affecting the particle size, the biologic-shell mimicking NPs with dense coverage of negative and positive charges were thus attained and their physicochemical parameters are shown in Table 1. Surface charge reversal was noticed with PGA addition and a decreased insulin EE was found attributed to the electrostatic competition. Besides, particle size of the w/o SA (merely PGA adding) group was similar to the PGA-free one, implying a negligible influence on NPs size beyond the transformation of charge after PGA addition. Intriguingly, a pronounced decrease in particle size and a higher EE were observed after SA combination in the SA/CS-Biotin$_{21.8\%}$ group (Table 1). A reliable explanation regarding that is SA coverage with high density leads to the formation of a solid protein shell on the exterior, which is responsible for a compacted structure of NPs and the screen of electrostatic interaction. To demonstrate the above statement, morphology of the biologic-shell mimicking NPs was observed by TEM. As seen in Fig. 2D, a visible protein capsid structure for SA/CS-Biotin$_{21.8\%}$ was validated and noted by yellow arrow.

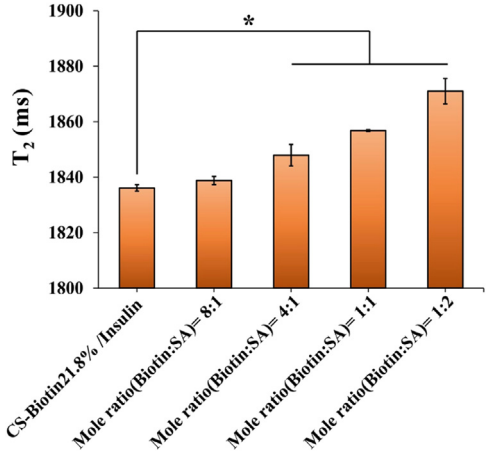

Fig. 1 – Comparisons of T_2 among insulin loaded NPs with different mole ratios of biotin and SA ($n = 3$). *$P < 0.05$ compared to CS-Biotin$_{21.8\%}$/Insulin.

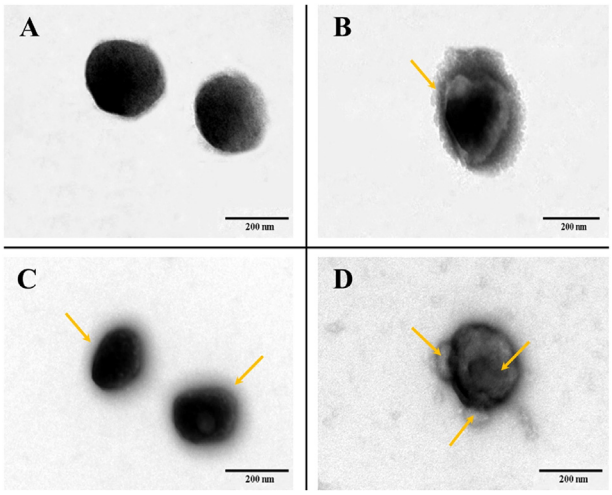

Fig. 2 – TEM images of (A) CS-Biotin$_{21.8\%}$/Insulin nanocomplexes; (B) HA/CS-Biotin$_{21.8\%}$;(C) Alg/CS-Biotin$_{21.8\%}$;(D) SA/CS-Biotin$_{21.8\%}$ (scale bar = 200 nm).

Table 1 – Physicochemical characteristics of the investigated nanoparticles.

Formulations	Particle size (nm)	Polydispersity index	Zeta potential (mV)	EE (%)
CS-Biotin$_{21.8\%}$/Insulin (Nanocomplex core)	195.4 ± 1.6	0.15 ± 0.02	16.25 ± 1.45	89.72 ± 0.52
w/o SA (without streptavidin combination)	192.1 ± 5.7	0.07 ± 0.02	−32.10 ± 0.90	69.42 ± 0.40
SA/CS-Biotin$_{21.8\%}$ (biologic-shell mimicking)	178.0 ± 6.4*	0.12 ± 0.02	−30.40 ± 0.90	80.82 ± 0.50*
HA/CS-Biotin$_{21.8\%}$ (polymeric-shell mimicking)	277.0 ± 12.7	0.06 ± 0.02	−27.90 ± 0.23	71.72 ± 0.48
Alg/CS-Biotin$_{21.8\%}$ (polymeric-shell mimicking)	237.7 ± 12.3	0.13 ± 0.04	−29.80 ± 1.72	74.40 ± 0.09

* $P < 0.05$ compared to the w/o SA group, *viz.*, merely PGA adding to the nanocomplex core.

For the counterpart of NPs based on polymeric-shell mimicking, prior study proved that structures of coating materials played a major role in mucus penetrating ability beyond surface charge of NPs, with Alg (MW = 145 kDa, 37%–40% G content) and HA (MW = 200 kDa) presented better effect [9,10]. Hence, on the basis of the nanocomplex core, NPs based on polymeric-shell mimicking were constructed by previously optimized HA or Alg coating. The increased particle size and decreased surface charge suggested the formation of a thicker polymer coating layer on the surface of the nanocomplex core. Among them, the particle size of HA/CS-Biotin$_{21.8\%}$ was significantly larger than Alg/CS-Biotin$_{21.8\%}$ (Table 1), whereas the higher-charged Alg coating produced NPs with a modest increase in size [23]. Moreover, the comparable zeta potential and EE were seen albeit their varying surface structure. TEM images stated a clearly defined core-shell structure for HA-coated NPs, whereas a distinctive halo-like appearance was seen on NPs with Alg coating (Fig. 2A–2C, noted by the yellow arrow). The nanocomplex core, on the other hand, was spherical or sub-spherical in shape and around 200 nm in size.

Collectively, the overall particle size of polymeric-shell mimicking NPs (around 300 nm) was significantly greater than that of NPs biologic-shell based, which is nevertheless appropriate for oral drug delivery [24]. It should be noted that within the particle size range of ~200 or 230–280 nm, the limited spatial blocking of the slime determined the muco-permeability of NPs was more affected by their surface properties [25,26]. Therefore, the size of two types of virus-mimicking NPs could be seen as in the same magnitude. Additionally, coupled with the comparable surface potential of about −30 mV, which is considered optimum for NP stability [27], the parallel comparison system was thus established to better understand the impact of virus-capsid mimicking NPs with varying structural features on a series of subsequent performance.

3.2. *Stability of virus-capsid mimicking NPs with different structure*

It is acknowledged that stability of NPs is intensely subject to pH microenvironment and tenacious peptidase, determining the fate of oral NPs. Herein, the colloid stability and trypsin resistance of virus-capsid mimicking NPs were analyzed and displayed in Fig. 3. Considering NPs based on polysaccharide as the main skeleton are vulnerable to harsh stomach environment due to swelling and ions exclusion, which could be surmounted by film coating or encapsulation [17], therefore, the colloidal stability of the virus-capsid mimicking NPs was investigated by incubating them in SIM and examining their size characteristics prior interacting with intestinal mucus. It was found that, in pH 6.8 SIM, no discernible change in particle size was noticed for different virus-capsid mimicking NPs despite a slight increase of particle size in polymer (HA/Alg) coated NPs group ($P > 0.05$), demonstrating their favorable colloid stability in a simulated intestinal milieu (Fig. 3A).

Following that, ability of the NPs to protect insulin from tryptic degradation was examined further (Fig. 3B). Compared with CS-Biotin$_{21.8\%}$/Insulin, the enzymatic stability of w/o SA was greatly improved due to the introduction of PGA functioning as a cross-linking agent enabling enhanced stability of the nanocomplex core [28], with further improvement after SA combination (appr. 30% insulin remaining after 2 h). Moreover, polymeric-shell mimicking NPs revealed comparable stability against trypsin, indicating the shell structure difference stemmed from various polymer coating didn't influence the shielding effect of insulin. Overall, two types of virus-capsid mimicking NPs could provide insulin with an appreciable and similar level of protection, which is advantageous for the subsequent epithelial cellular uptake, transport of NPs and a better comparison of the contribution of virus-capsid mimicking NPs with different structure on *in vivo* absorption.

3.3. *Influence of virus-capsid mimicking NPs with different structure on mucus diffusion*

Mucus, which is widely distributed throughout the gastrointestinal tract, plays an important role in protecting the body from xenobiotics invasion to prevent dysfunction. However, the turnover mucus layer is also a natural barrier for NPs transport. Therefore, overcoming mucus trapping is a prerequisite for subsequent uptake by intestinal cells for oral nano-delivery systems. First, we incubated two types of virus-capsid mimicking NPs with mucin for up to 3 h. No significant change was observed in particle size of the NPs-mucin compound during incubation (Fig. 4A), indicating that NPs did not dissociate, allowing NPs to remain intact after crossing the mucus barrier. Next, to investigate the muco-penetration performance of different virus-capsid mimicking NPs, a reliable approach was applied using crude porcine mucus *in vitro*. As shown in Fig. 4B, compared to CS-Biotin$_{21.8\%}$/Insulin, significantly improved mucus permeability of the NPs was achieved after PGA addition ($P < 0.05$), with a 1.4-fold enhancement, attributing to PGA imparted NPs electronegative property, thereby

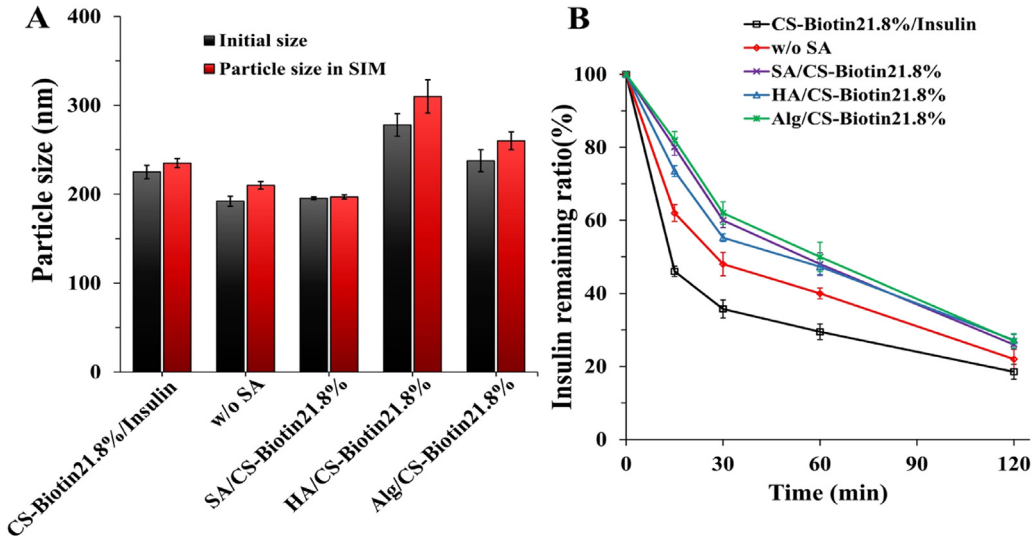

Fig. 3 – (A) The colloidal stability of investigated NPs after incubation in simulated intestinal medium for up to 2 h. (B) Enzymatic stability of investigated NPs in the presence of trypsin (250 U/ml).

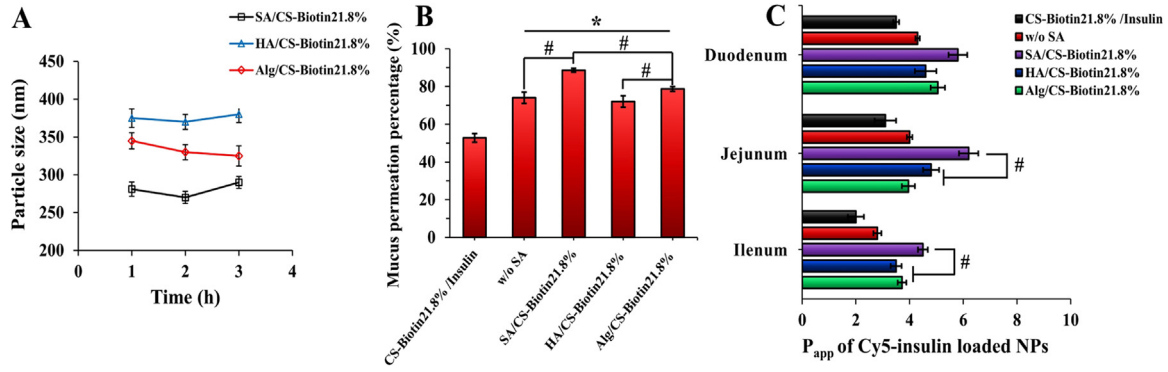

Fig. 4 – (A) The variation of the particle size during the incubation of formulations with Type II mucin. (B) Overall muco-permeation percentage of FITC-insulin loaded NPs. (C) Apparent permeability coefficient of various Cy5-insulin loaded NPs in different intestinal segments of rats ($n = 3$). *$P < 0.05$ compared to CS-Biotin$_{21.8\%}$/Insulin, $^{\#}P < 0.05$ compared to the indicated group.

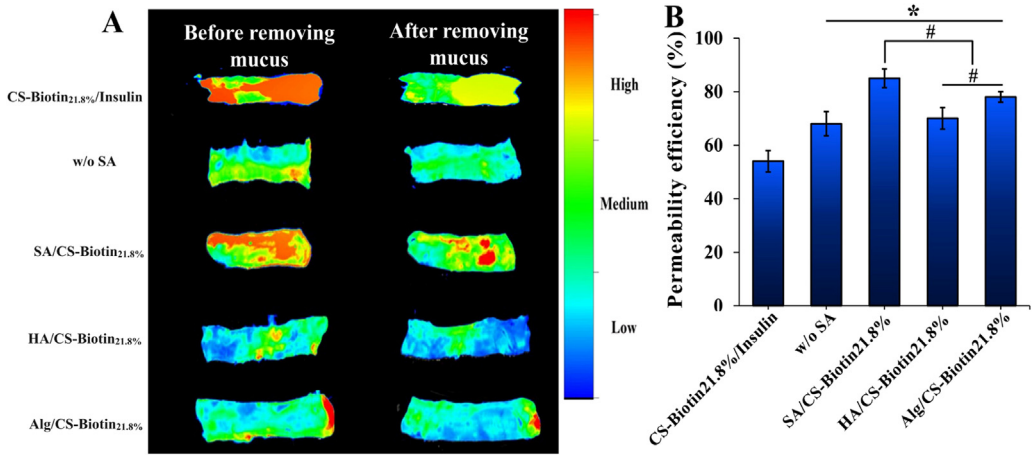

Fig. 5 – The intestinal retention reflected by the fluorescence intensity of Cy5-insulin loaded NPs in jejunum of rats. (A) Living imaging. (B) Semi-quantitative analysis of the results. *$P < 0.05$ compared to CS-Biotin$_{21.8\%}$/Insulin, $^{\#}P < 0.05$ compared to the indicated group.

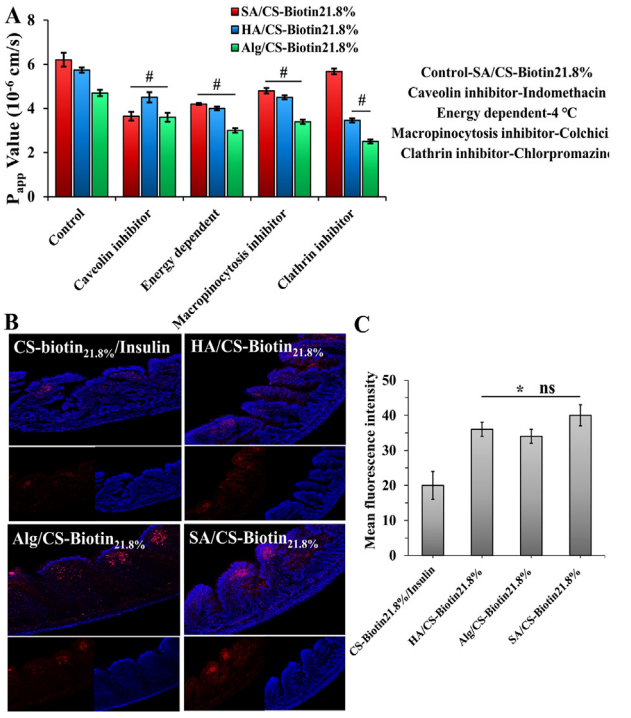

Fig. 6 – (A) The apparent permeability coefficient of different structured virus-capsid mimicking NPs in presence of various uptake inhibitors. (B) Visualization of virus-capsid mimicking biologic-shell based versus polymeric-shell based NPs being absorbed by villi in jejunum. (C) Semiquantitative analysis of fluorescence intensity by Image J software. ($n = 3$, $^{\#}P < 0.05$ *versus* the control group, $^{*}P < 0.05$ compared to CS-Biotin$_{21.8\%}$/Insulin, ns indicates no significant differences between groups).

preventing interaction with negatively charged mucin and facilitating the penetration of NPs through the mucus layer. Furthermore, a further improvement was realized upon SA combination (14% increase versus w/o SA group), owing to the fact that hydrophilic SA contains a high fraction of non-glycosylated domains than avidin that lessens the hydrophobic interaction with porcine mucus [11,29]. Regarding the polymeric-shell mimicking ones, HA and Alg coated NPs showed a 1.4- and 1.7-fold improvement compared to CS-Biotin$_{21.8\%}$/Insulin respectively. Besides, NPs coated by Alg, whose structure was characterized by low guluronic acid (G) content and low molecular weight [10], reflected a greater permeation percentage than those coated by HA, but it was still inferior to the SA/CS-Biotin$_{21.8\%}$ group ($P < 0.05$).

In general, although the virus-capsid mimicking NPs with different structure featured comparable particle size and zeta potential (Table 1), they displayed different permeation enhancing capacities, telling the structure of capsid-mimicking based on biologic-shell and polymeric-shell could shape the interaction between NPs and mucus as well.

3.4. *Influence of virus-capsid mimicking NPs with different structure on intestinal permeation*

Apart from mucus lining, the underlying intestinal epithelium is another major obstacle that NPs have to encounter subsequently before entering into the systemic circulation. Hence, the permeation of various virus-capsid mimicking NPs was comparatively studied in duodenum, jejunum and ileum of rats *in vitro*. Compared to CS-Biotin$_{21.8\%}$/Insulin, a considerably elevated P_{app} value was observed for SA/CS-Biotin$_{21.8\%}$, with a 1.6- to 2.2-fold increase in the intestinal regions (Fig. 4C), which was echoing the above *in vitro* mucus diffusion results (Fig. 4B). By contrast, w/o SA group exhibited inappreciable permeation enhancement in the small intestine compared with CS-Biotin$_{21.8\%}$/Insulin. Moreover, SA/CS-Biotin$_{21.8\%}$ exhibited significantly enhanced permeation improvement in jejunum and ileum compared with the polymeric-shell mimicking NPs ($P < 0.05$). Among them, Alg/CS-Biotin$_{21.8\%}$ appeared to be less effective than HA/CS-Biotin$_{21.8\%}$ at improving permeability in the jejunum, which may result from the chelation between HA and tight junction-related calcium ions [30,31]. Additionally, it was shown that P_{app} value was also impacted by the intestinal segments (jejunum > duodenum >> ileum) in addition to the surface feature of virus-mimicking NPs, which matched the thickness of mucus in each segment (170 μm, 123 μm and 480 μm, respectively) [32].

Taken together, designing functionalized virus-capsid mimicking NPs based on polymer coating or protein components envelope was advantageous to enhance intestinal trans-mucus and transmucosal penetration efficiency but the benefit was structure dependent, with SA covered NPs revealing the best performance.

3.5. *Ex vivo muco-penetration study*

For further comparison and visualization of the muco-penetrating situation in context of approaching real-world *in vivo* circumstances, the penetration effectiveness of varied virus-capsid mimicking NPs was evaluated in *ex vivo* mucus via assessing the intestinal retention both before and after mucus removal. *N*-acetyl-L-cysteine (NAC), as a mucolytic agent was utilized in this study to clean out the mucus lining. As shown in Fig. 5A, before NAC disposing, the nanocomplex core exhibited a strong FI owing to the bioadhesive attribute of CS as a skeleton, while the reduced FI of w/o SA group was found upon the addition of PGA (fluorescence intensity from red to blue-green), resulting in the system translation from mucoadhesion to muco-penetration. After NAC treating, the FI of CS-Biotin$_{21.8\%}$/Insulin was significantly attenuated, suggesting majority of positively charged nanocomplexes adhered to loose mucus layer could be cleared by mucus removal. Notably, even after mucus elimination, SA/CS-Biotin$_{21.8\%}$ remained a greater FI, indicating more particles reached the underlying unstirred water layer. In contrast, both NPs coated by HA or Alg remained to have a moderate FI after NAC processing. Further semi-quantitative analysis of the permeability percentage of the various formulations is depicted in Fig. 5B, compared to CS-Biotin$_{21.8\%}$/Insulin, two types of virus-capsid mimicking NPs were capable

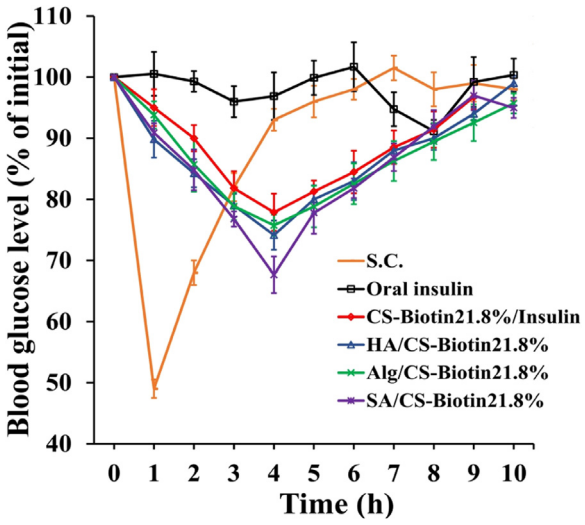

Fig. 7 – Profiles of the hypoglycemic level following administration of different NPs ($n = 6$).

of enhancing penetration in jejunum, with SA covered NPs being the most efficacious. Furthermore, between the polymer (HA/Alg) coated NPs with different surface structure, Alg coated NPs appeared to be more effective than NPs with HA coating, matching the *in vitro* mucus permeation results displayed in Fig. 4B. Although the initial FI of virus-capsid mimicking NPs with different structure was lower than CS-Biotin$_{21.8\%}$/Insulin with good mucoadhesion, the drop in FI was not substantial before and after mucus elimination. The summative outcomes were reflected by permeability efficiency profiles of NPs whereas SA/CS-Biotin$_{21.8\%}$ > Alg/CS-Biotin$_{21.8\%}$ > HA/CS-Biotin$_{21.8\%}$ ≈ w/o SA > CS-Biotin$_{21.8\%}$/Insulin (Fig. 5B).

3.6. *Study of enterocyte endocytosis pathways and visualization*

To gain a deeper understanding of the enterocyte internalization mechanism, we conducted a study employing the jejunum as a representative model of the intestine. Our objective was to probe the impact of various endocytosis inhibitors on the intestinal absorption of virus-capsid mimicking NPs. As shown in Fig. 6A, the P_{app} value of SA/CS-Biotin$_{21.8\%}$ was reduced by 34% after being incubated with a caveolin inhibitor (indomethacin), indicating that caveolin-mediated endocytosis was engaged in the process of absorption. Moreover, the greatly reduced P_{app} was seen at 4 °C, suggesting the intestinal transport of SA/CS-Biotin$_{21.8\%}$ also relied on energy. By contrast, inferring from the reduction extent of P_{app} value in the presence of chlorpromazine, the NPs with polymer (HA/Alg) coating was mainly involved in clathrin-mediated multiple endocytosis pathway (Fig. 6A). It was reported that the NPs ingested by caveolae pathway could evade lysosome capture and endosome hydrolysis, and experienced a lower extent of drug degradation unlike those by clathrin endocytic pathway, which could facilitate drug absorption into blood [33]. Therefore, together with the aforementioned mucodiffusion and intestinal transport studies (Figs. 4C and 5), the superior penetration efficiency of SA/CS-Biotin$_{21.8\%}$ in entrails was well demonstrated again in virtue of the caveolin-mediated endocytosis process, with multiple uptake mechanisms implicated. Based on these results, it could be concluded that caveolin-mediated endocytosis was more beneficial to NPs transport across enterocytes compared to clathrin-mediated passage, which could be manipulated by biologic-shell formation via SA coverage.

Given that the absorption of NPs was reliant on the intestinal segments as indicated by the intestinal permeability results, with the jejunum segment showing the best absorption site of formulations (Fig. 4C), herein, *in situ* absorption of the virus-capsid mimicking NPs with diverse surface traits in jejunum was visualized by confocal laser scanning microscopy to further verify the *ex vivo* results. As shown in Fig. 6B, the weaker FI was found in the control group because of the strong mucus-nanocomplex interaction and poor uptake, thereby mostly situated on the marginal villi. By contrast, the virus-capsid mimicking NPs allowed more Cy5-insulin to be absorbed by enterocytes out of which SA/CS-Biotin$_{21.8\%}$ enabled more NPs to distribute into deep folded microvilli by virtue of its stronger trans-mucus and trans-epithelial delivery efficiency, which was consistent with the aforementioned results of mucus diffusion and intestinal permeation. However, there were no significant differences among the virus-capsid mimicking NPs (Fig. 6C), so further *in vivo* absorption test is essential to comparatively study the overall biological effect.

3.7. *Study of in vivo hypoglycemic behavior*

Finally, the *in vivo* hypoglycemic behavior of healthy rats was evaluated to elucidate the influence of virus-capsid mimicking NPs based on different structure with improved muco-penetration and diverse endocytosis mechanisms on *in vivo* efficacy. As seen in Fig. 7, all investigated groups showed a degree of hypoglycemic level whereas free insulin group had an invalid influence on the blood glucose level, indicating virus-capsid mimicking NPs design is efficacious in enhancing oral insulin absorption. The reduction of blood glucose level occurred within 4 h after virus-capsid mimicking NPs were administrated, which showed a swift and sustained hypoglycemic effect. For the two polymeric-shell mimicking NPs, they presented comparable hypoglycemic profiles, with the lowest glucose level around 74% at 4 h, both of them showed better therapeutic efficiency compared to the CS-Biotin$_{21.8\%}$/Insulin group (Table 2). By comparison, NPs with SA coverage displayed the highest hypoglycemic impact, with the blood glucose level decreasing to almost 67% and a relative PA of 5.1%, in line with the *in vitro* and *ex vivo* data. This investigation confirmed once more that *in vivo* insulin extent post oral administration was virus-capsid structure dependent, with biologic-shell mimicking NPs based on protein components via SA coverage helped to improve insulin absorption to a large extent than polymer coated virus-mimicking NPs.

We next assessed the *in vivo* safety of formulations post oral administration on the basis of histological analysis. After 7-d oral treatment, no histological abnormalities or hyperemia

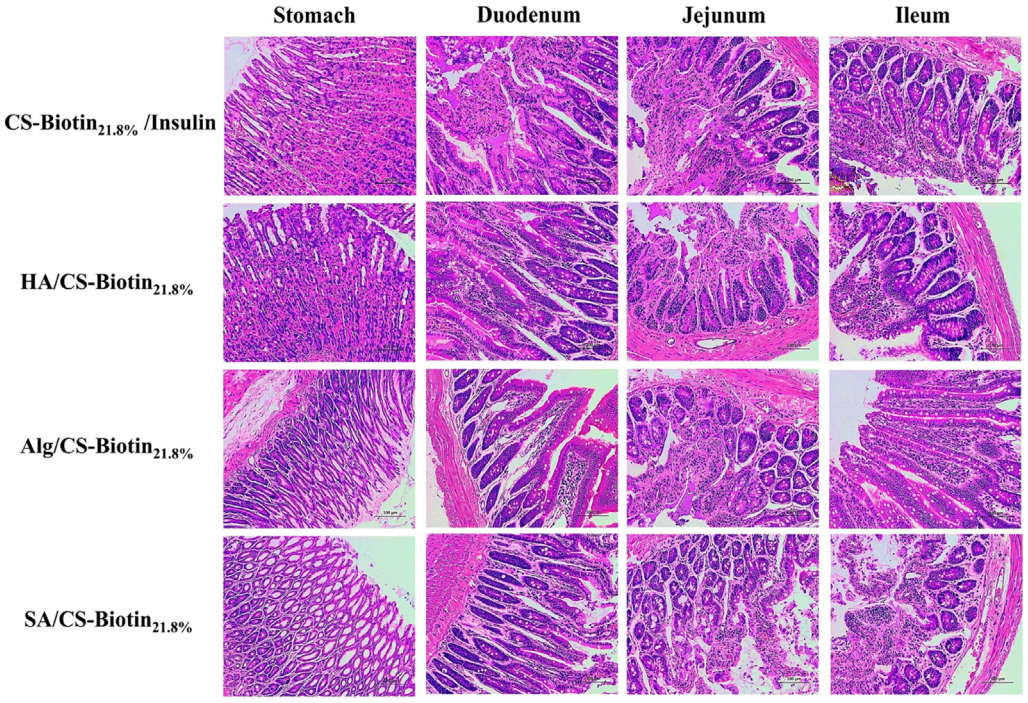

Fig. 8 – Gastrointestinal irritation evaluation after the oral administration of different formulations at a dose of 50 IU/kg for 7 days.

Table 2 – Relative pharmacological availability of different insulin samples for male SD rats following administration ($n = 6$).

Formulation	Administration route	Dosage (IU/kg)	T_{max} (h)	AAC (%*h)	Relative pharmacological bioavailability (%)
Free insulin	Oral	50	–	–	–
Free insulin	Injection	2	1	123	100
CS-Biotin$_{21.8\%}$/Insulin	Oral	50	4	113	3.8 ± 0.4
HA/CS-Biotin$_{21.8\%}$	Oral	50	4	138	4.6 ± 0.3
Alg/CS-Biotin$_{21.8\%}$	Oral	50	4	140	4.5 ± 0.4
SA/CS-Biotin$_{21.8\%}$	Oral	50	4	147	5.1 ± 0.3*

* $P < 0.05$ compared to CS-Biotin$_{21.8\%}$/Insulin.

were found (Fig. 8), indicating benign tissue biocompatibility of these drug delivery systems.

4. Conclusion

To elucidate the impact of different virus-capsid mimicking structure for enhanced oral insulin delivery, using CS-Biotin$_{21.8\%}$ as the main skeleton, virus-mimicking NPs with polymer (HA, Alg) coating or SA coverage utilizing biotin-SA interaction were rationally developed herein, followed with a systematical comparison regarding *in vitro* and *in vivo* properties. It was demonstrated that improved penetration efficiency of NPs across mucus lining and small intestine was in a virus-capsid mimicking structure dependent manner, with SA/CS-Biotin$_{21.8\%}$ revealing the best performance. The endocytic pathway study proved that caveolin-mediated endocytosis mainly contributed to the absorption of SA covered NPs compared to that of polymer coated NPs with a clathrin-mediated passage, which was more conducive for the transport of NPs across enterocytes. *In vivo* study revealed that the insulin absorption extent of the NPs was virus-capsid structure dependent, with biologic-shell mimicking NPs exhibiting the most effective curative effect. In summary, the external composition of virus-capsid mimicking NPs can influence the mucodiffusion capacity and transmembrane mechanism, thereby determining the absorption extent, which should be well taken into consideration. Furthermore, virus-mimicking NPs endowed with biologic-shell based on protein components via SA coverage were a promising prototype delivery platform for enhanced oral insulin. Despite the beneficial outcomes, they do not guarantee that the hypoglycemic effect can be achieved clinically, more *in vivo* experiments need to be further investigated and explored in the future.

Conflicts of interest

The authors declare no conflict of interest.

Acknowledgement

The authors gratefully acknowledge financial support from National Natural Science Foundation of China (grant no. 31870987).

References

[1] Bhardwaj M, Yadav P, Dalal S, Kataria SK. A review on ameliorative green nanotechnological approaches in diabetes management. Biomed Pharmacother 2020;127:110198.
[2] Iyer G, Dyawanapelly S, Jain R, Dandekar P. An overview of oral insulin delivery strategies (OIDS). Int J Biol Macromol 2022;208:565–85.
[3] Wu R, Wu Z, Xing L, Liu X, Wu L, Zhou Z, et al. Mimicking natural cholesterol assimilation to elevate the oral delivery of liraglutide for Type II diabetes therapy. Asian J Pharm Sci 2022;17(5):653–65.
[4] Liu C, Kou Y, Zhang X, Cheng H, Chen X, Mao SR. Strategies and industrial perspectives to improve oral absorption of biological macromolecules. Expert Opin Drug Deliv 2018;15(3):223–33.
[5] Date AA, Hanes J, Ensign LM. Nanoparticles for oral delivery: design, evaluation and state-of-the-art. J Control Release 2016;240:504–26.
[6] Bandi SP, Bhatnagar S, Venuganti VVK. Advanced materials for drug delivery across mucosal barriers. Acta Biomater 2021;119:13–29.
[7] Shin K, Suh H, Grundler J, Lynn AY, Pothupitiya JU, Moscato ZM, et al. Polyglycerol and poly(ethylene glycol) exhibit different effects on pharmacokinetics and antibody generation when grafted to nanoparticle surfaces. Biomaterials 2022;287:121676.
[8] Netsomboon K, Bernkop-Schnürch A. Mucoadhesive *vs.* mucopenetrating particulate drug delivery. Eur J Pharm Biopharm 2016;98:76–89.
[9] Cui ZX, Qin L, Guo S, Cheng HB, Zhang X, Guan J, et al. Design of biotin decorated enterocyte targeting muco-inert nanocomplexes for enhanced oral insulin delivery. Carbohydr Polym 2021;261:117873.
[10] Zhang X, Cheng HB, Dong W, Zhang M, Liu Q, Wang X, et al. Design and intestinal mucus penetration mechanism of core-shell nanocomplex. J Control Release 2018;272:29–38.
[11] Jain A, Cheng K. The principles and applications of avidin-based nanoparticles in drug delivery and diagnosis. J Control Release 2017;245:27–40.
[12] Marques AC, Costa PJ, Velho S, Amaral MH. Functionalizing nanoparticles with cancer-targeting antibodies: a comparison of strategies. J Control Release 2020;320:180–200.
[13] Mao SR, Bakowsky U, Jintapattanakit A, Kissel T. Self-assembled polyelectrolyte nanocomplexes between chitosan derivatives and insulin. J Pharm Sci 2006;95(5):1035–48.
[14] Liu C, Kou Y, Zhang X, Dong W, Cheng H, Mao SR. Enhanced oral insulin delivery via surface hydrophilic modification of chitosan copolymer based self-assembly polyelectrolyte nanocomplex. Int J Pharm 2019;554:36–47.
[15] Karamanidou T, Karidi K, Bourganis V, Kontonikola K, Kammona O, Kiparissides C. Effective incorporation of insulin in mucus permeating self-nanoemulsifying drug delivery systems. Eur J Pharm Biopharm 2015;97:223–9.
[16] Meng Q, Tian L, Wang J. Random amphiphilic copolymeric sub-micro particles as a carrier shielding from enzymatic attack for peptides and proteins delivery. J Mater Sci: Mater Med 2012;23(4):991–8.
[17] Cui ZX, Liu C, Cui SM, Qin L, Zhang X, Guan J, et al. Exploring the potential of redispersible nanocomplex-in-microparticles for enhanced oral insulin delivery. Int J Pharm 2022;612:121357.
[18] Jacob D, Joan TM, Tomlins P, Sahota TS. Synthesis and identification of FITC-insulin conjugates produced using human insulin and insulin analogues for biomedical applications. J Fluoresc 2016;26(2):617–29.
[19] Cheng HB, Zhang X, Qin L, Huo Y, Cui ZX, Liu C, et al. Design of self-polymerized insulin loaded poly(n-butylcyanoacrylate) nanoparticles for tunable oral delivery. J Control Release 2020;321:641–53.
[20] Tian H, He Z, Sun C, Yang C, Zhao P, Liu L, et al. Uniform core-shell nanoparticles with thiolated hyaluronic acid coating to enhance oral delivery of insulin. Adv Healthc Mater 2018;7(17):1800285.
[21] Liu M, Zhang J, Zhu D, Shan W, Li L, Zhong JJ, et al. Efficient mucus permeation and tight junction opening by dissociable "mucus-inert" agent coated trimethyl chitosan nanoparticles for oral insulin delivery. J Control Release 2016;222:67–77.
[22] Sakahara H, Saga T. Avidin–biotin system for delivery of diagnostic agents. Adv Drug Deliv Rev 1999;37(1):89–101.
[23] Sadat HM, Kamali B, Nabid MR. Multilayered mucoadhesive hydrogel films based on Ocimum basilicum seed mucilage/thiolated alginate/dopamine-modified hyaluronic acid and PDA coating for sublingual administration of nystatin. Int J Biol Macromol 2022;203:93–104.
[24] He C, Yin L, Tang C, Yin C. Size-dependent absorption mechanism of polymeric nanoparticles for oral delivery of protein drugs. Biomaterials 2012;33(33):8569–78.
[25] Lock JY, Carlson TL, Carrier RL. Mucus models to evaluate the diffusion of drugs and particles. Adv Drug Deliv Rev 2018;124:34–49.
[26] Lai SK, Wang Y, Hanes J. Mucus-penetrating nanoparticles for drug and gene delivery to mucosal tissues. Adv Drug Deliv Rev 2009;61(2):158–71.
[27] Cacua K, Ordoñez F, Zapata C, Herrera B, Pabón E, Buitrago-Sierra R. Surfactant concentration and pH effects on the zeta potential values of alumina nanofluids to inspect stability. Colloids Surf A Physicochem Eng Asp 2019;583:123960.
[28] Su F, Lin K, Sonaje K, Wey S, Yen T, Ho Y, et al. Protease inhibition and absorption enhancement by functional nanoparticles for effective oral insulin delivery. Biomaterials 2012;33(9):2801–11.
[29] Schechter B, Silberman R, Arnon R, Wilchek M. Tissue distribution of avidin and streptavidin injected to mice. Eur J Biochem 1990;189(2):327–31.
[30] Gao C, Zhang M, Ding J, Pan F, Jiang Z, Li Y, et al. Pervaporation dehydration of ethanol by hyaluronic acid/sodium alginate two-active-layer composite membranes. Carbohydr Polym 2014;99:158–65.
[31] Hagesaether E. Permeation modulating properties of natural polymers – effect of molecular weight and mucus. Int J Pharm 2011;409(1–2):150–5.
[32] Ensign LM, Cone R, Hanes J. Oral drug delivery with polymeric nanoparticles: the gastrointestinal mucus barriers. Adv Drug Deliv Rev 2012;64(6):557–70.
[33] Zheng Y, Wu J, Shan W, Wu L, Zhou R, Liu M, et al. Multifunctional nanoparticles enable efficient oral delivery of biomacromolecules via improving payload stability and regulating the transcytosis pathway. ACS Appl Mater Interfaces 2018;10(40):34039–49.